

Active Vibration Control Using Piezostack Based Mount

압전작동기 마운트를 이용한 능동진동제어

Vien-Quoc Nguyen, Sang-Min Choi, Yong-Seok Paeng, Young-Min Han,
Seung-Bok Choi and Seok-Jun Moon

벤 큐 오* · 최 상 민* · 팽 용 석* · 한 영 민** · 최 승 복† · 문 석 준***

(2007년 10월 2일 접수 ; 2008년 1월 9일 심사완료)

Key Words : Hybrid Mount(하이브리드 마운트), Piezostack Actuator(압전작동기), Feed-forward Control
(앞먹임 제어기)

ABSTRACT

This paper presents active vibration control performance of a hybrid mount. The proposed hybrid mount is devised by adopting both piezostack as an active actuator and rubber as a passive element. After experimentally identifying actuating force characteristics of the piezostack and dynamic characteristics of the rubber, the hybrid mount was designed and manufactured. Subsequently, a vibration control system with a specific mass loading is constructed, and its governing equations of motion are derived. In order to actively attenuate vibration transmitted from the base, a feedforward controller is formulated and experimentally realized. Vibration control responses are then evaluated in time and frequency domains.

요 약

이 논문에서는 하이브리드 마운트의 능동진동제어 성능에 대하여 기술하였다. 제안된 하이브리드 마운트는 압전작동기의 능동요소와 고무의 수동요소로 구성하였다. 압전작동기의 작동력 특성과 고무의 동적 특성을 실험적으로 구하여 이를 바탕으로 하이브리드 마운트를 설계 및 제작 하였다. 그리고 특정 질량을 결합한 진동제어 시스템을 구축하고, 그 시스템의 지배 방정식을 수립하였다. 지면으로부터 전달되는 진동을 능동적으로 절연시키기 위해서 앞먹임 제어기를 구축하고 실험적으로 구현하였다. 그리고 가속도, 힘 전달력 등 진동 제어 성능을 시간과 주파수 영역에서 평가하였다.

1. Introduction

In general, mounts are used to attenuate shocks and vibrations of dynamic systems for

many applications such as naval equipment subjected to severe dynamic environments. Many types of the passive mounts have been used to achieve this purpose. A rubber mount is one type of passive mount which is widely used due to its efficient vibration isolation performance against non-resonant and high frequency excitation⁽¹⁾. However, the passive rubber mount cannot exert good performance at some frequency regions, especially at resonant

† 교신저자: 정회원, 인하대학교 기계공학부
E-mail : seungbok@inha.ac.kr

Tel : (032)872-7925, Fax : (032)868-1716

* 정회원, 인하대학교 대학원 기계공학과

** 정회원, 인하대학교 기계공학부

*** 정회원, 한국기계연구원 e-엔지니어링연구센터

frequencies. This performance limitation of the passive mount leads to the study on active and semi-active mounts featuring smart materials which include electro-rheological fluid^(2~4), magneto-rheological fluid⁽⁵⁾ piezoelectric materials^(6,7) and shape memory alloys⁽⁸⁾. Among these, the piezoelectric material is one of the most promising candidates because of its fast response and easy controllability. However, the approach to directly bond the piezoelectric actuator on structures is not effective for large-sized structures under severe vibration loading such as equipments installed in naval vessels.

The main objective of this work is to propose a new type of active hybrid mount which can operate in wide frequency range. In addition, its control performance is experimentally evaluated in an actual vibration system. The proposed active hybrid mount consists of one passive rubber element and two active piezostack actuators. After identifying material characteristics of the rubber element and the actuating force of the piezostack actuators, the hybrid mount was manufactured and applied to the vibration system with a lumped mass. The governing equations of motion of the proposed system are derived and followed by the synthesis of a simple feedforward control algorithm to attenuate vibrations from the base. In wide frequency range from 20 Hz to 1000 Hz, vibrations control performance is experimentally evaluated in time domain. In addition, transmitted forces are demonstrated in frequency domain.

2. Mount Configuration

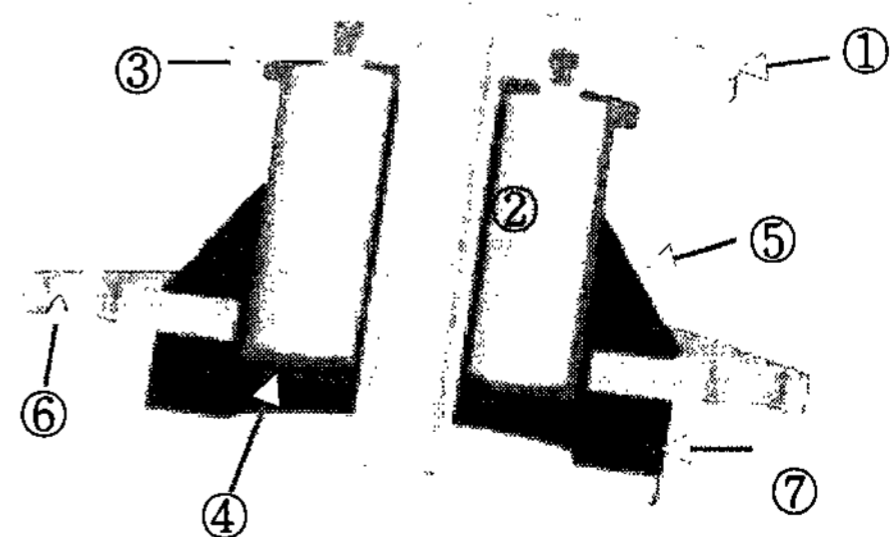
Figure 1 shows the configuration of the proposed hybrid mount which consists of piezostack actuators, rubber element and

intermediate mass. As shown in the figure, two piezostack actuators located in parallel are combined with the rubber element in serial connection to prevent severe excitation. It is noted that the proposed hybrid mount is very effective to severe dynamic environments with high shocks and vibrations, such as equipment installed in naval vessels.

In this work, a lumped mass is located on the top plate above the proposed mount. Excitations according to the military standard MIL-STD-167-1A shown in Table 1 are transmitted through the insert plate from the base below the mount. The system of the proposed mount and the supported mass ('mount-mass system' for short) can be modeled as a two degree-of-freedom(2-DOF) system. From the mechanical model of the proposed system shown in Fig. 2, the governing equations of motion can be derived as follows.

$$\begin{aligned} m_1 \ddot{x}_1(t) + c_1 \dot{x}_1(t) + (k_1 + 2k_2)x_1(t) \\ - k_2 x_2(t) = 2f_a(t) + c_1 \dot{x}_0(t) + k_1 x_0(t) \quad (1) \\ m_2 \ddot{x}_2(t) + 2k_2 x_2(t) - 2k_2 x_1(t) = -2f_a(t) \end{aligned}$$

where $x_1(t)$ and $x_2(t)$ are the displacement of the inertial mass and of the supported mass, respectively; x_0 is the displacement of the base (excitation); k_1 and c_1 are the stiffness and



- ① Top plate
- ② Piezostack actuator
- ③ Intermediate plate
- ④ Inertial mass
- ⑤ Rubber element
- ⑥ Insert plate
- ⑦ Center plate

Fig. 1 Configuration of the hybrid mount

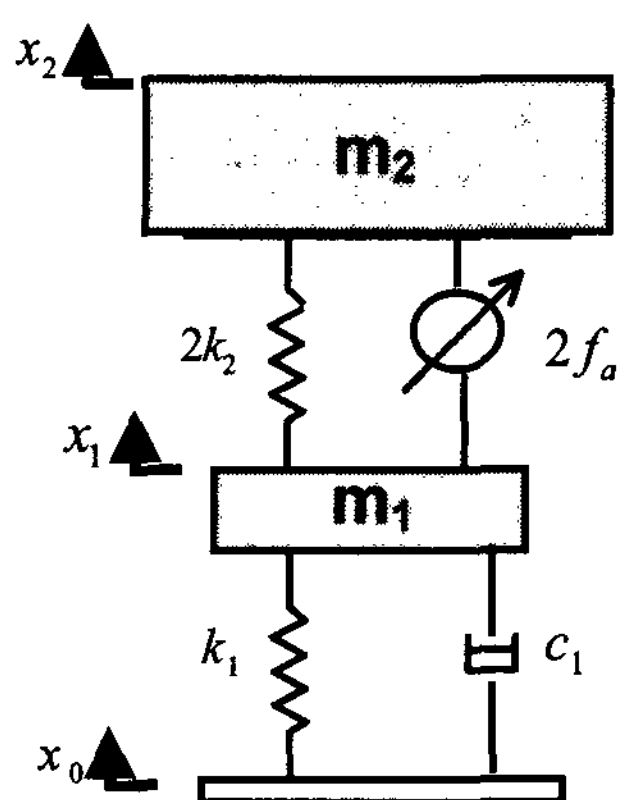


Fig. 2 Mechanical model of the hybrid mount

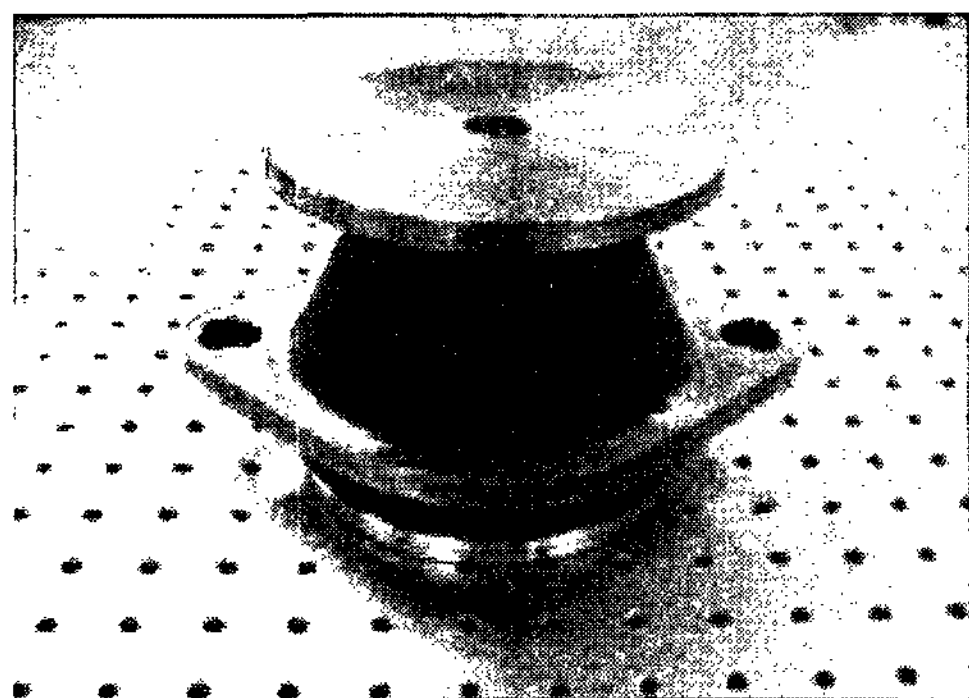


Fig. 3 A photograph of the manufactured hybrid mount

Table 1 Specification of MIL-STD-167-1A

Freq. (Hz)	20	50	100	200	500	1000
Acc. (m/s ²)	0.4737	1.1843	2.3687	4.7374	11.8435	23.6871

damping coefficient of the rubber element, respectively; k_2 in the stiffness of the piezostack actuators; $f_a(t)$ is the force exerted by the piezostack actuators. These parameters can be experimentally determined. The Fig. 3 shows the photograph of the manufactured hybrid mount. In this work, the mass m_1 and m_2 are chosen to be 1.7 kg and 50 kg, respectively.

3. Parameter Identification

The rubber element is designed and manu-

factured under consideration of mounting environments of the naval equipments. Its loading range is from 50 to 200 kg. In general, the characteristics of the rubber are changed in accordance with upper load and vibration source. Therefore, the dynamic stiffness and damping coefficient can be experimentally determined by using Kelvin-Voigt model as follows.

$$k_d(j\omega) = k_1 + j\omega c_1 \tag{2}$$

where k_d is dynamic stiffness, k_1 the static stiffness, c_1 the damping constant, and ω the excitation frequency. An experiment has been performed to determine the transmissibility of the rubber element, from which the stiffness and damping coefficients are determined by 160447 N/m and 537 Ns/m, respectively.

On the other hand, the electromechanical behavior of the piezostack, providing actuation along the polarized direction, can be expressed as follows.

$$D = \epsilon_{33}E + d_{33}T \tag{3}$$

$$S = d_{33}E + \frac{1}{c}T \tag{4}$$

In the above, D is the electrical displacement, E the electric field, T the stress, S the strain, ϵ_{33} the dielectric constant at zero stress, d_{33} the piezoelectric charge constant, and c the elastic modulus at zero electric field. Then the constitutive equation of the piezostack actuator stack by n layers can be derived from the equation as follows.

$$\begin{aligned} f_p(t) &= AT = AcS - Acd_{33}E \\ &= Ac \frac{\delta(t)}{l} - Acd_{33} \frac{V(t)}{l} \\ &= k_p \delta(t) - \alpha V(t) = k_p \delta(t) - f_a(t) \end{aligned} \tag{5}$$

where $f_p(t)$ is the load applied to the

piezostack, A the cross-sectional area of the piezoelectric element, l the length of the piezostack, $k_p (= Ac/l)$ the spring constant, $a (= Acd_{33}/l)$ the proportional constant, and $f_a(t) (= \alpha V(t))$ the force exerted by the input voltage $V(t)$. The stroke $\delta(t)$ of the piezostack can be predicted from the following equation.

$$\delta(t) = \frac{1}{k_p} [\alpha V(t) + f_p(t)] \quad (6)$$

Figure 4 presents experimental results of blocking force produced by the piezostack actuators. The average value of the spring constant and proportional constant of the piezostack actuators is 47 MN/m and 2.4 N/V, respectively. The maximum blocking force is evaluated by 1000 N at the input voltage of 300 V. The results also show that the two piezostack actuators have nearly the same stiffness. Figure 5 shows the measured actuating force with respect to the frequency. It is observed that the force increases proportionally to the square of the frequency.

4. Controller Design

In this work, control purpose is to suppress vibration of the supported mass transmitted from the base. By defining a state vector $\mathbf{x} = [x_1 \ x_2 \ \dot{x}_1 \ \dot{x}_2]^T$, the governing equations of the mount-mass system (1) can be rewritten in state-space representation as follows

$$\begin{aligned} \dot{\mathbf{x}}(t) &= \mathbf{A}\mathbf{x}(t) + \mathbf{B}u(t) + \mathbf{\Gamma}d(t), \quad z(t) = \mathbf{C}\mathbf{x}(t) \\ y(t) &= \dot{z}(t) \end{aligned} \quad (7)$$

where $z(t)$ and $y(t)$ is the velocity and the acceleration of the supported mass m_2 respectively; the input $u(t)$ is voltage applied to the piezostack actuators; $d(t) \triangleq c_1 \dot{x}_0(t) + k_1 x_0(t)$ is disturbance which excites from the base. The matrices \mathbf{A} , \mathbf{B} , \mathbf{C} , and $\mathbf{\Gamma}$ are given by

$$\begin{aligned} \mathbf{A} &= \begin{bmatrix} 0 & 0 & 1 & 0 \\ 0 & 0 & 0 & 1 \\ \frac{-(k_1 + 2k_2)}{m_1} & \frac{2k_2}{m_1} & \frac{-c_1}{m_1} & 0 \\ \frac{2k_2}{m_2} & \frac{-2k_2}{m_2} & 0 & 0 \end{bmatrix} \\ \mathbf{B} &= \begin{bmatrix} 0 \\ 0 \\ \frac{2\alpha}{m_1} \\ \frac{-2\alpha}{m_2} \end{bmatrix}, \quad \mathbf{\Gamma} = \begin{bmatrix} 0 \\ 0 \\ \frac{-1}{m_1} \\ 0 \end{bmatrix} \\ \mathbf{C} &= [0 \ 0 \ 0 \ 1] \end{aligned} \quad (8)$$

The feedforward controller is formulated as follows.

$$u(t) = -\mathbf{K}d(t) \quad (9)$$

where \mathbf{K} is the control gain. By substituting Eq. (9) into Eq. (7), we obtain

$$\dot{\mathbf{x}}(t) = \mathbf{A}\mathbf{x}(t) + (\mathbf{\Gamma} - \mathbf{B}\mathbf{K})d(t) \quad (10)$$

It would be ideal if we can make $(\mathbf{\Gamma} - \mathbf{B}\mathbf{K}) = 0$, in which there would be absolutely no influence of the disturbance $d(t)$ on the system. Unfortunately, in our system, since the number of inputs is less than that of the states, there is no selection of \mathbf{K} which results in $(\mathbf{\Gamma} - \mathbf{B}\mathbf{K}) = 0$. However, \mathbf{K} can be chosen to minimize the effect of the disturbance $d(t)$. In our case, since d and u are scalars, \mathbf{K} must be scalar. Hence it can be tuned easily to obtain the best value in practice. Figure 6 shows the corresponding control block diagram of the proposed control system.

5. Control Results and Discussions

Figure 7 shows the experimental setup for vibration control. A 50 kg mass is loaded on the upper plate of the mount, while the insert plate

is excited by an electromagnetic shaker. Two accelerometers are used: one is installed on the shaker to measure the acceleration of the vibration source for feedforward control; the other is installed on the mass to monitor its vibration for evaluating the control performance.

The controller is implemented by using dSPACE DSP board DS1104, in which the high-speed A/D and D/A converters are integrated. The sampling rate of the control

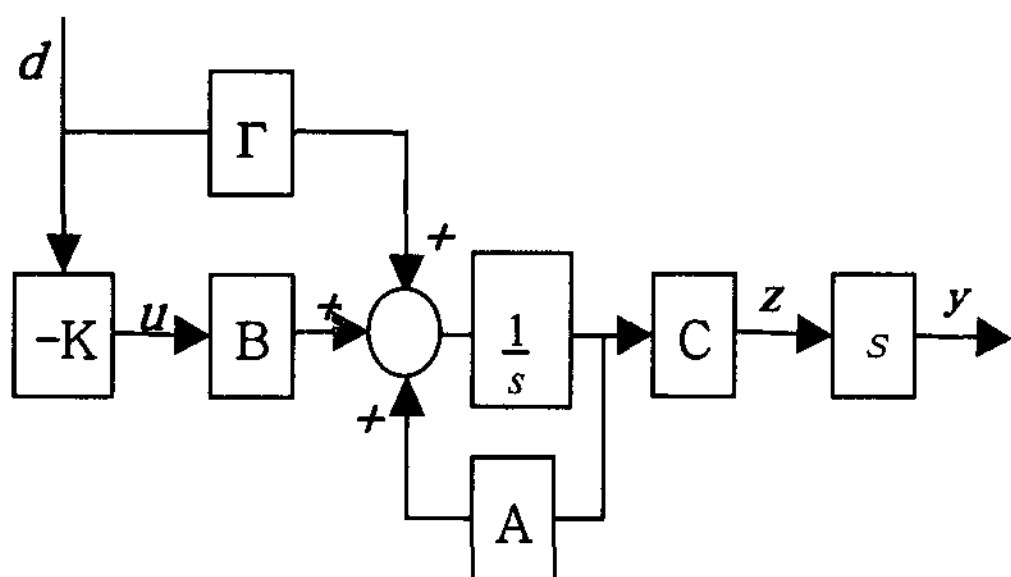
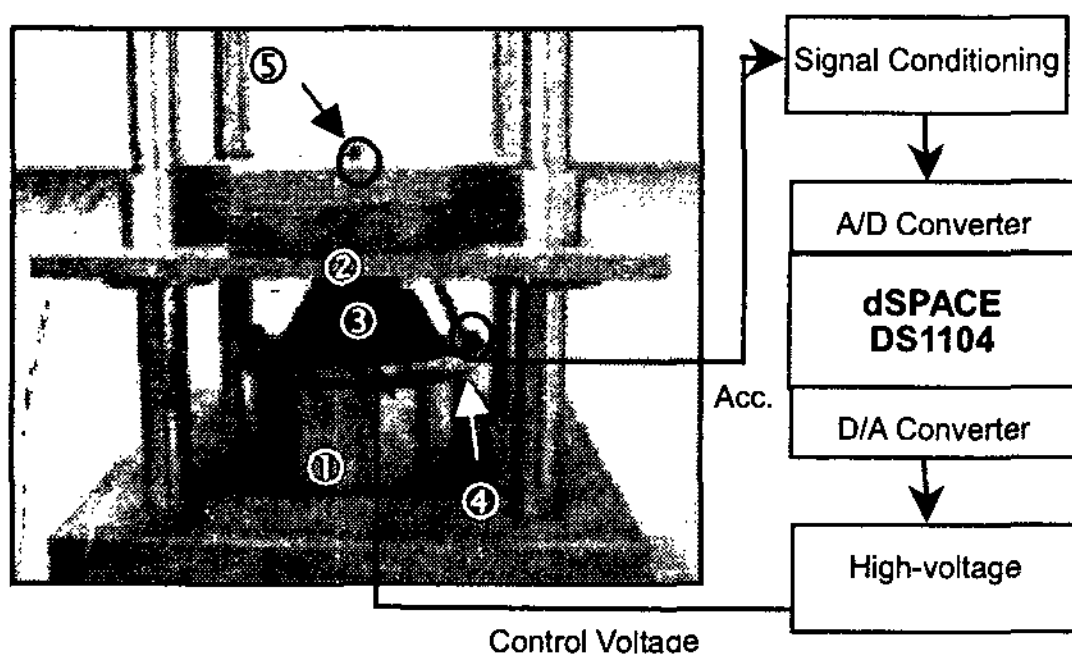


Fig. 6 Block diagram of the control system



- ① Shaker + Jig
- ② 50 kg mass
- ③ Hybrid mount
- ④,⑤ Accelerometers

Fig. 7 Experimental apparatus for vibration control

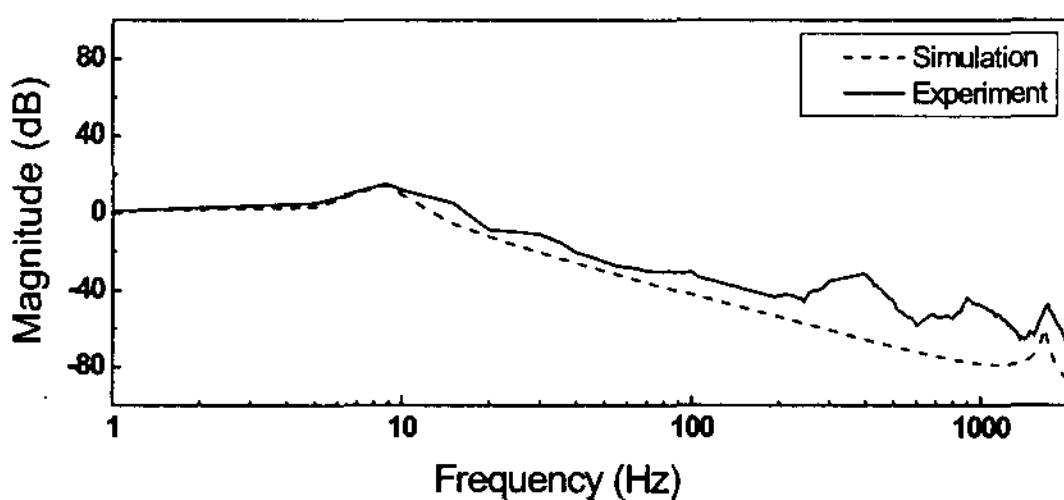


Fig. 8 Frequency response of the mount-mass system

system is chosen to be 10 kHz. When the vibration is transmitted to the mount, the feedforward controller is activated to attenuate the vibration at the supported mass. The dynamic response signals are acquired from accelerometers at the supported mass and shaker via dSPACE DSP board DS1104. Figure 8 shows the measured frequency response of the mount-mass system. From the simulation result, two resonant frequencies are found at 8.78 Hz and 1.2 kHz which are the same as the measured ones. It is also seen that there are two resonant peaks at 400 Hz and 900 Hz in the experimental result.

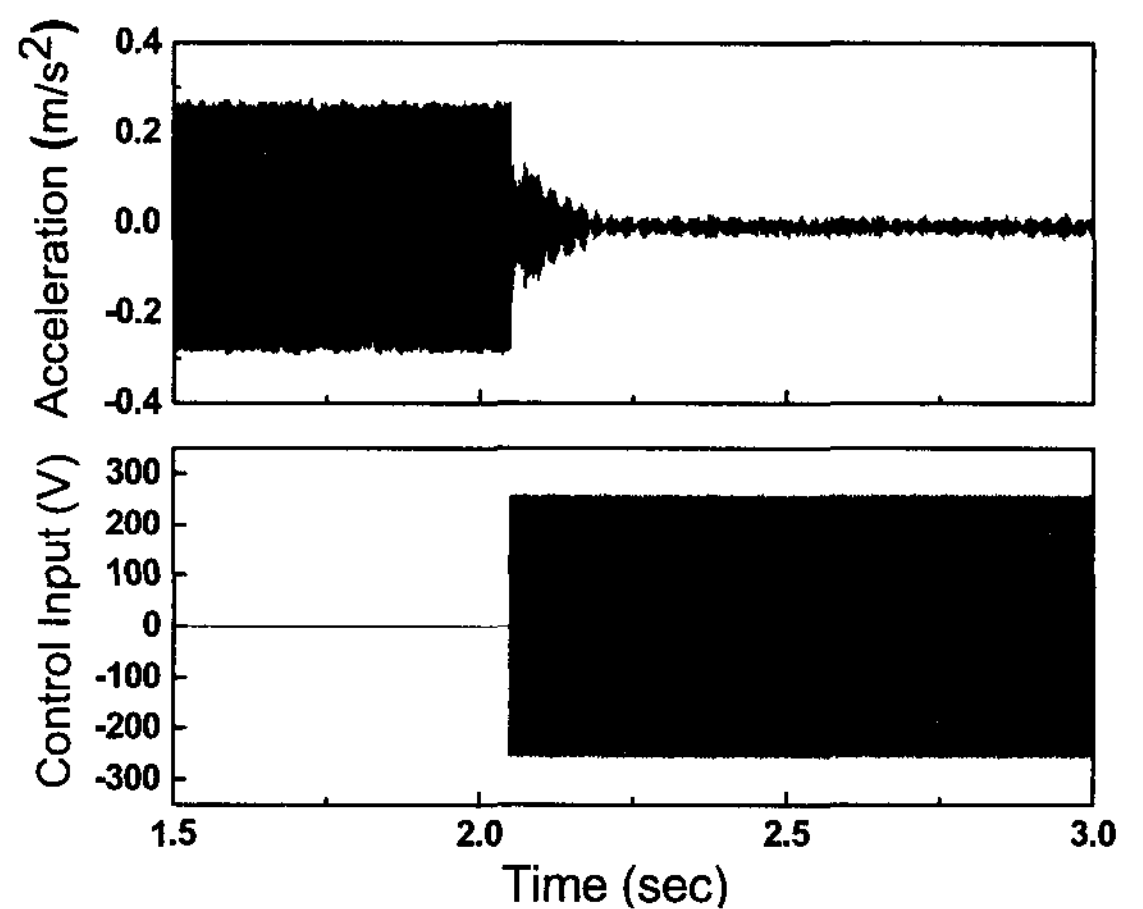


Fig. 9 Control response under excitation at 400 Hz

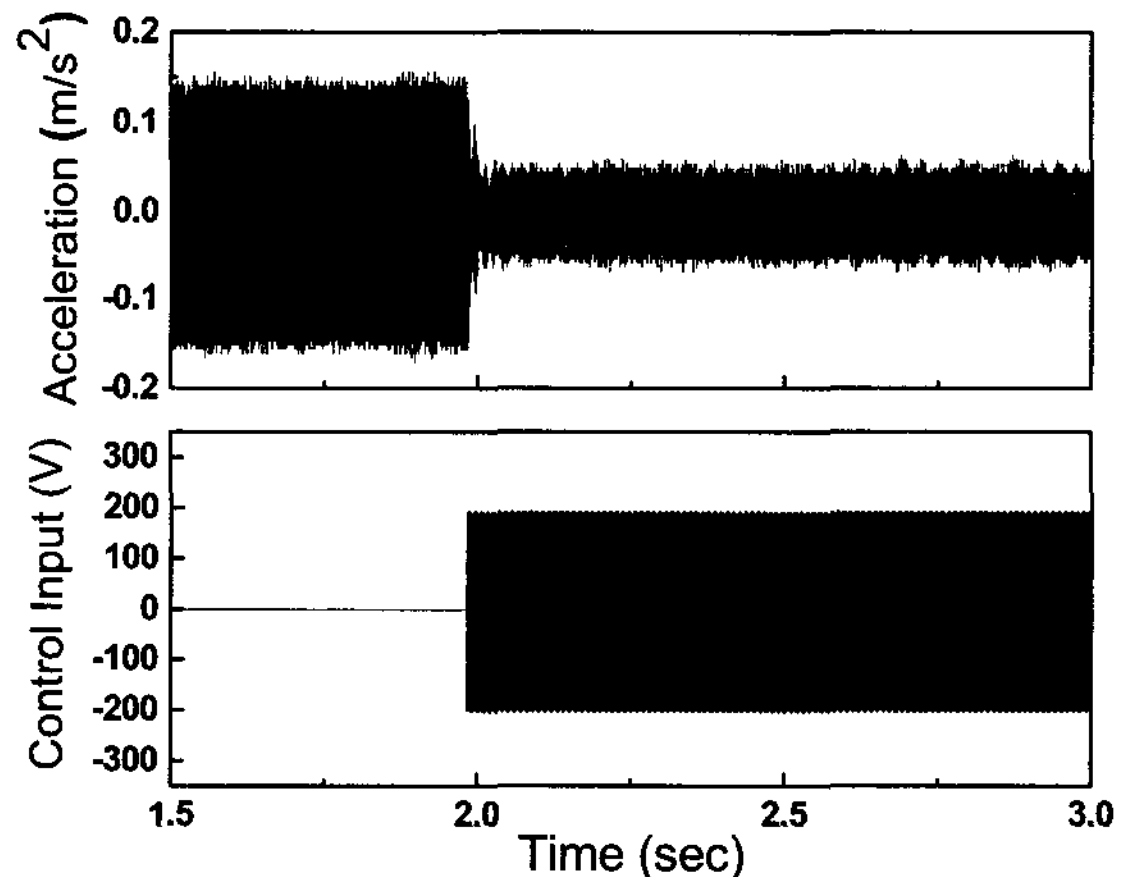


Fig. 10 Control response under excitation at 900 Hz

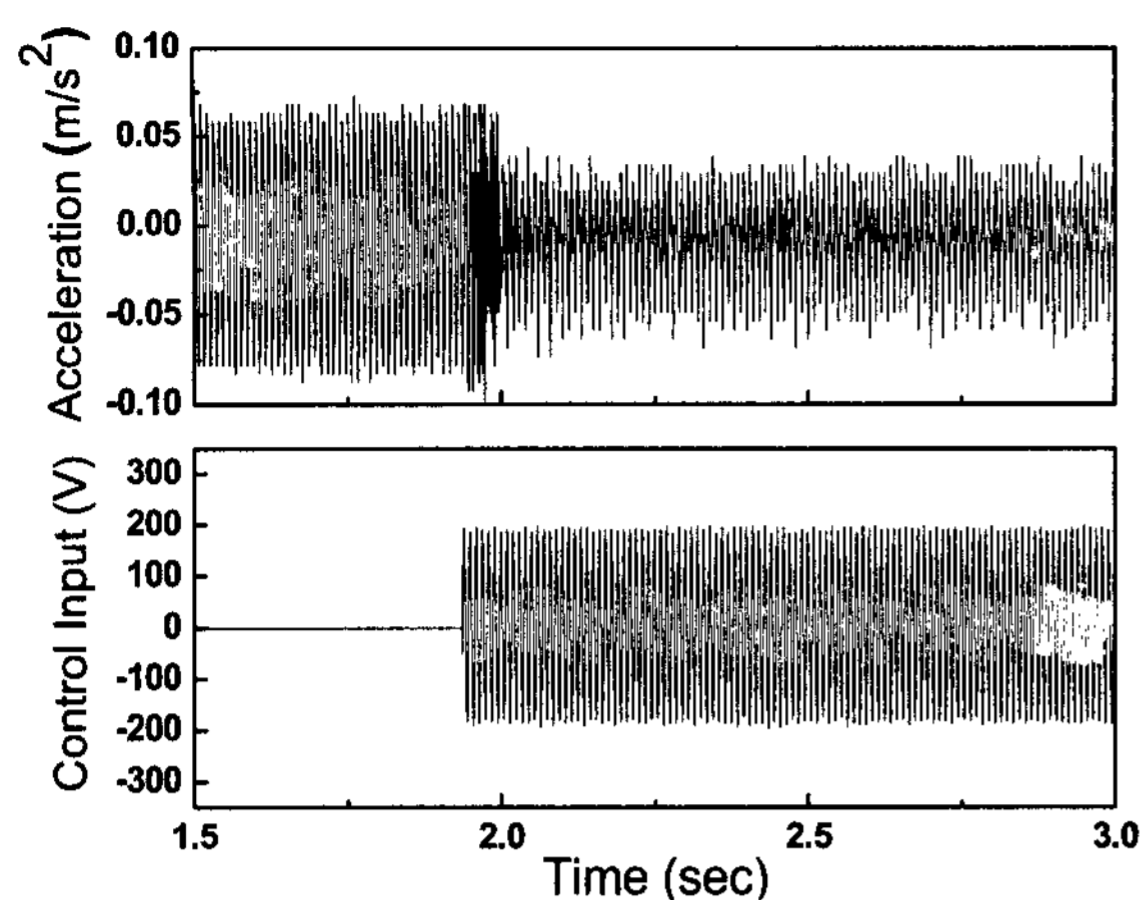


Fig. 11 Control response under excitation at 100 Hz

In the first vibration control experiment, the shaker is set to generate sinusoidal vibration at 400 Hz with amplitude of $1.69 \mu\text{m}$. The corresponding excitation acceleration is 10.68 m/s^2 . Time response of the system is shown in Fig. 9. When the controller is not activated, the vibration at the mass is suppressed to 0.27 m/s^2 or -31.86 dB . The corresponding maximum displacement and transmitted force are $0.0432 \mu\text{m}$ and 13.64 N , respectively. After 2.05 seconds, the controller is activated. It can be seen that the acceleration is effectively reduced to 0.0152 m/s^2 or -56.94 dB in total (compared with the excitation). The corresponding displacement and transmitted force are reduced to $0.0024 \mu\text{m}$ and 0.76 N , respectively. The vibration of the mass in controlled case is 25.08 dB lower than that in uncontrolled case. Figure 10 presents the control performance under high frequency excitation at 900 Hz . From the experimental results, it can be seen that acceleration of the supported mass is decreased 9.42 dB by activating the proposed feedforward controller. In the low frequency at 100 Hz , the vibration attenuation is favorable as shown in Fig. 11.

Table 2 presents the attenuated vibration levels in a wide frequency range from 20 to 1000 Hz . The column (b) shows the excitation according to the MIL spec.; the column (c) and

Table 2 Experimental results at several frequencies

Freq (Hz)	Excit- ation (m/s^2)	Uncontrolled		Controlled		Attenuated level (dB)
		Acc. (m/s^2)	Dec. level (dB)	Acc. (m/s^2)	Dec. level (dB)	
(a)	(b)	(c)	(d)	(e)	(f)	(g)=f-d
20	0.47	0.157	-8.75	0.147	-9.33	-0.58
50	1.18	0.049	-9.89	0.041	-11.44	-1.55
70	1.66	0.049	-30.70	0.047	-31.06	-0.36
100	2.37	0.075	-30.54	0.028	-39.10	-8.56
200	4.74	0.048	-40.21	0.029	-44.64	-4.43
300	7.11	0.128	-35.15	0.018	-52.16	-17.01
400	9.47	0.273	-31.86	0.015	-56.94	-25.08
500	11.84	0.062	-45.94	0.013	-59.54	-13.60
600	14.21	0.016	-58.72	0.004	-70.55	-11.83
700	16.58	0.036	-53.89	0.024	-57.46	-3.57
800	18.95	0.040	-54.56	0.015	-63.13	-8.57
900	21.32	0.147	-43.34	0.050	-52.76	-9.42
1000	23.69	0.092	-47.54	0.022	-59.84	-12.30

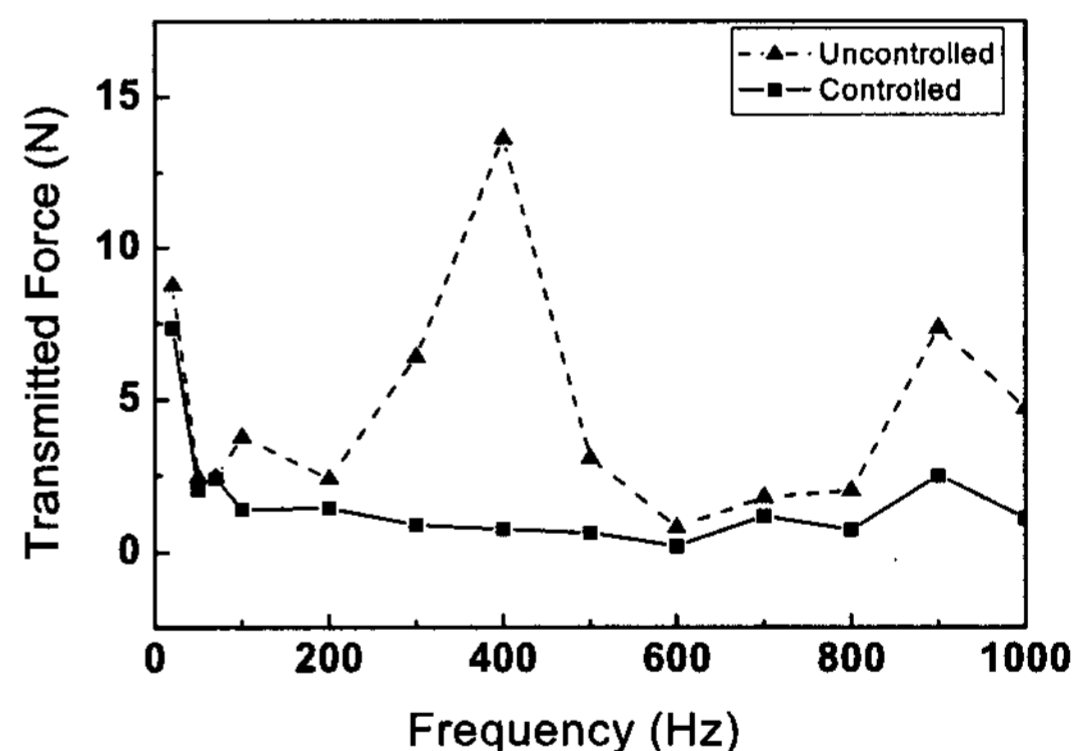


Fig. 12 Transmitted force in frequency domain

(e) show the acceleration at the mass m_2 in uncontrolled and controlled cases respectively; the column (g) shows the attenuated level of the controlled case compared with the uncontrolled case. The corresponding transmitted force is demonstrated in Fig. 12. From these results, it can be assured that the vibration control performance of the proposed hybrid mount is superior in a wide frequency range. It is also noted that control performance below

100 Hz is relatively low because of small inertial force of the piezostack actuator by low frequency excitation. The experimental results show that by using the proposed hybrid mount with a proper controller, the vibration isolating performance can be effectively achieved in a wide frequency range. It is also observed that the control performance at resonant frequencies (400 Hz and 900 Hz) is much remarkable compared to non-resonant frequency range.

6. Conclusions

In this paper, an active hybrid mount has been proposed for equipment subjected to severe dynamic environment such as naval vessels. By adopting piezostack actuators and rubber element, the proposed mount was designed and manufactured. A simple feed-forward controller was formulated to suppress vibrations of a 50 kg mass in a mount-mass system. Through experimental realization of the feedforward control, it has been demonstrated that the imposed vibrations were substantially reduced in a wide frequency range from 20 Hz to 1000 Hz.

Acknowledgements

This work was supported by Dual Technology Project. This financial support is gratefully acknowledged.

References

- (1) Yunhe, Y., Nagi, G. N. and Rao, V. D., 2001, "A Literature Review of Automotive Vehicle Engine Mounting Systems", *Mechanism and Machine Theory*, Vol. 36, pp. 123~142.
- (2) Hong, S. R., Choi S. B., Jung, W. J., Ham, I. B. and Kim, D. K., 2001, "Vibration Control of an ER Mount Subjected to High Static Loads", *Journal of Sound and Vibration*, Vol. 242, No. 4, pp. 740~748.
- (3) Choi, S. H., Choi, Y. T., Choi, S. B. and Cheong, C. C., 1996, "Performance Analysis of an Engine Mount Featuring ER Fluids and Piezoactuators", *International Journal of Modern Physics B*, Vol. 10, No. 23, pp. 3143~3157.
- (4) Jung, W. J., Jeong, W. B., Hong, S. R. and Choi, S. B., 2004, "Vibration Control of a Flexible Beam Structure Using Squeeze-mode ER Mount", *Journal of Sound and Vibration*, Vol. 273, pp. 185~199.
- (5) Hong, S. R. and Choi, S. B., 2005, "Vibration Control of a Structural System Using Magneto-rheological Fluid Mount", *Journal of Intelligent Material Systems and Structures*, Vol. 16, pp. 931~936.
- (6) Kim, S. H., Choi, S. B., Hong, S. R. and Han, M. S., 2004, "Vibration Control of a Flexible Structure Using a Hybrid Mount", *International Journal of Mechanical Sciences*, Vol. 46, pp. 143~157.
- (7) Choi, S. B., Hong, S. R. and Kim, S. H., 2004, "Beam Vibration Control via Rubber and Piezostack Mounts: Experimental Work", *Journal of Sound and Vibration*, Vol. 273, pp. 1079~1086.
- (8) Choi, S. B. and Cheong, C. C., 1996, "Vibration Control of a Flexible Beam Using SMA Actuators", *Journal of Guidance, Control, and Dynamics*, Vol. 19, No. 5, pp. 1178~1180.
- (9) Yook, J. Y., Choi, S. B., Sung, K. G. and Moon, S. J., 2007, "Design of Hybrid Mount Using Rubber Element and Piezoelectric Actuator with Application to Vibration Control", *Transactions of the Korean Society for Noise and Vibration Engineering*, Vol. 17, No. 5, pp. 390~397.
- (10) Paeng, Y. S., Yook, J. Y. and Choi, S. B., Moon, S. J., 2007, "Control Performance of Hybrid Mount Using Electromagnetic Actuator and PZT Actuator", *Transactions of the Korean Society for Noise and Vibration Engineering*, Vol. 17, No. 7, pp. 617~623.